

Chapter 3

Hafnene on Ir(111)



Abstract Two-dimensional (2D) honeycomb systems made of elements with d electrons are rare. In this chapter, we report the fabrication of a transition metal (TM) 2D film, namely, hafnium (Hf) monolayer on Ir(111). Experimental characterizations reveal that the Hf layer possesses honeycomb lattice, morphologically identical to graphene. First-principles calculations provide evidence for directional bonding between adjacent Hf atoms, analogous to carbon atoms in graphene. Calculations further suggest that the freestanding Hf honeycomb could be ferromagnetic with magnetic moment $\mu/\text{Hf} = 1.46 \mu\text{B}$. The realization and investigation of TM honeycomb layers extend the scope of 2D structures and could bring about novel properties for technological applications.

Keywords Hafnium · Honeycomb structure · Transition metal · STM · LEED · Ir(111)

3.1 Background

The novel properties of graphene's honeycomb structure have spurred tremendous interest in investigating other two-dimensional (2D) layered structures beyond graphene. This includes, for example, hexagonal boron nitride [1–3], silicene [4–10], and germanene [11]. Almost exclusively, however, the reported 2D honeycomb materials are made of elements with p-orbital electronic structure [12, 13]. The 2D honeycomb structures made of elements with d electrons are still rare, although there are many more transition metal (TM) elements than the ordinary main group honeycomb elements in the first two rows of the Periodic Table. Generally, the TM elements have rich many-body physical behaviors and coordination chemistry properties; many of them also exist as spin-polarized magnetic ions. Hence, it is highly desirable to fabricate 2D honeycomb structures of the TM elements for drastically enhanced and novel electronic, spintronic, and catalytic activities.

3.2 Preparation and STM Study

In the present work, we challenge the conventional wisdom that honeycomb structure can exist only in elements that bear high chemical similarity to carbon. We report that the honeycomb structure of TM elements can also be fabricated with totally uncharted physics and chemistry in particular for Hf on Ir substrate [14]. Low-energy electron diffraction (LEED) and scanning tunneling microscopy (STM) measurements reveal that despite the triangular planar structure of the substrate Hf forms its own honeycomb structure with Hf–Hf nearest neighbor distance remarkably close to that of bulk Hf. Electronic structure calculation further reveals the direct bonding of covalent character between the nearest neighboring Hf atoms, as reflected in the calculated total charge density.

Experiments were carried out in our UHV-MBE-STM system. The Ir(111) single crystal was cleaned by several cycles of Ar⁺ ion sputtering followed by annealing at around 1473 K until sharp 1×1 diffraction spots in the LEED pattern and clean surface terraces in the STM images were obtained. Hf atoms, evaporated from the electron-beam evaporator, were deposited at room temperature. The Hf flux was set at 10 nA. The deposition time varied depending on the intended Hf coverage. The sample was subsequently annealed until a well-ordered structure was observed. The STM and LEED techniques were combined to characterize the structural and physical properties of the Hf/Ir system. First-principles calculations were performed using the projector augmented wave (PAW) method as implemented in the Vienna ab initio simulation package (VASP) [15, 16]. The generalized gradient approximation of Perdew, Burke, and Ernzerhof (PBE) was used for the exchange and correlation interaction between electrons [17]. Periodic slabs with four layers of (4×4) Ir(111) were used as the substrate, plus one layer of Hf and a vacuum of 12 Å wide. All atoms were fully relaxed except for the bottom Ir layer until the net force on each atom was less than 0.01 eV/Å. The energy cutoff for the plane-wave basis set is 400 eV, and the k-points sampling is $3 \times 3 \times 1$. To simulate the STM images, we used the Tersoff-Hamann approach.

More specifically, we evaporated Hf atoms onto the clean Ir(111) surface, which, as seen in Fig. 3.1a, formed nanoclusters at room temperature. With follow-up annealing at 673 K, a well-ordered structure was observed in Fig. 3.1b. The structural information of the sample was then characterized by LEED. For comparison, Fig. 3.1c shows a typical LEED pattern of the clean substrate, in which the six spots result from the 6-fold symmetry of the Ir(111). After the deposition of Hf followed by annealing, additional diffraction spots appeared, as indicated by the red arrow in Fig. 3.1d, which signals that a new superstructure of Hf origin has emerged. It has the (2×2) pattern with respect to the Ir(111) substrate. The LEED data thus suggest the formation of a well-ordered network of Hf adlayer with a periodicity twice that of Ir(111).

To gain an understanding of this Hf superstructure in real space, we carried out an STM study. Figure 3.2a shows a typical STM image, which reveals a continuous 2D lattice of the honeycomb structure. The orientation of the honeycomb lattice

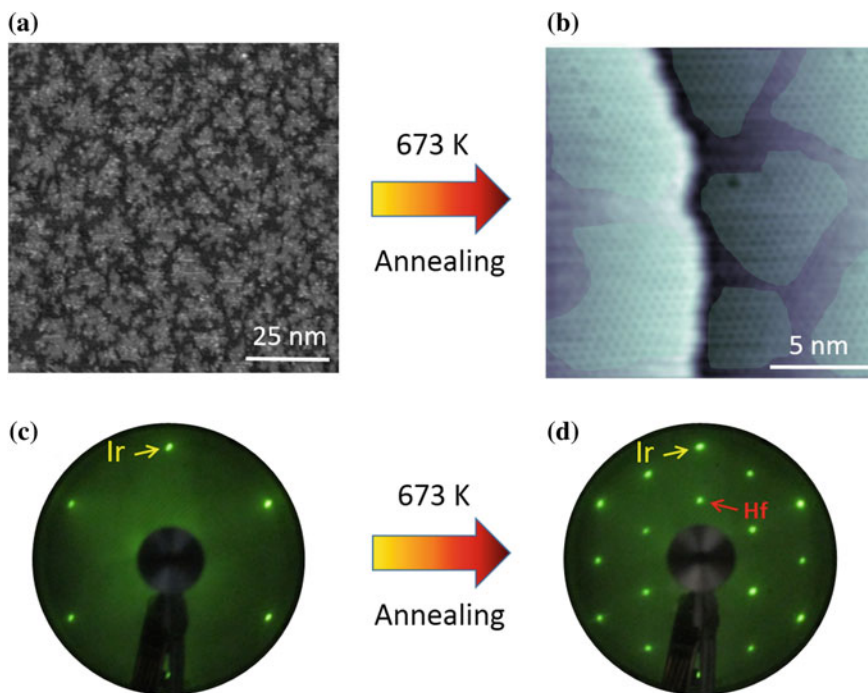


Fig. 3.1 Fabrication of Hafnene on Ir(111). **a** STM morphology of Hf clusters deposited on Ir(111) surface at room temperature ($U = -2.0$ V and $I = 0.2$ nA). **b** Hafnene sheets formed by annealing the sample at 673 K ($U = -1.2$ V and $I = 0.5$ nA). LEED patterns of **c** the clean Ir(111) substrate and **d** the hafnene sample are obtained at electron beam energies of 68 and 70 eV, respectively. Adapted with permission from Ref. [14], © 2013 ACS

is parallel to the close-packed $[1\bar{1}0]$ direction of the Ir(111) lattice, in agreement with the LEED results, where the reciprocal vectors of the Ir spots are in line with those of the Hf spots (see Fig. 3.1d). Figure 3.2b is a zoomed-in image in which a perfect honeycomb structure can be clearly resolved. Combining the STM results with the LEED patterns, we conclude that well-ordered Hf honeycomb with a (2×2) superstructure has formed on Ir(111). Figure 3.2c shows a height profile of the honeycomb lattice along the blue line in Fig. 3.2b. It indicates a 5.40 Å periodicity of the honeycomb lattice, which is consistent with the value deduced from the (2×2) spots in the LEED pattern (5.40 Å $\approx 2 \times 2.71$ Å, where 2.71 Å is the lattice constant of the Ir(111)). From this periodicity, we determine the distance between two adjacent Hf atoms in the 2D plane to be $(5.40/\sqrt{3})$ Å = 3.12 Å. This value is very close to the Hf–Hf distance of 3.19 Å on the (0001) facet of bulk Hf. Half of the value, 3.12 Å/2 = 1.56 Å, is also within the range of the proposed covalent radii for Hf, which are between 1.44 and 1.75 Å. In other words, the Hf atoms are the nearest neighbors, rather than disjointed adatoms on Ir(111).

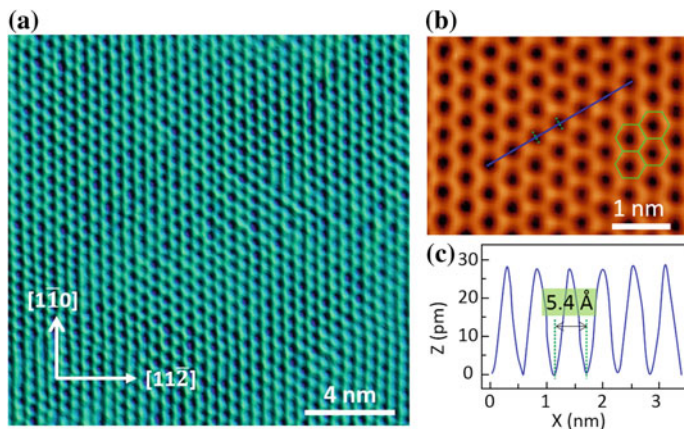


Fig. 3.2 STM images and height profile of Hf layer formed on Ir(111). **a** The topographic image ($U = -1.02$ V and $I = 0.80$ nA) shows a well-ordered pattern. The close-packed directions of Ir[1 $\bar{1}$ 0] and [1 1 $\bar{2}$] are indicated by the white arrows. **b** The close-up image ($U = -0.70$ V and $I = 0.16$ nA) shows the honeycomb lattice of the Hf adlayer. **c** A height profile taken along the blue line in (b), revealing the periodicity of the honeycomb lattice (5.4 Å between holes). Reproduced with permission from Ref. [14], © 2013 ACS

3.3 Theoretical Calculations of Atomic and Electronic Structures

To confirm the experimental observations, we conducted density functional theory (DFT) calculations. For isolated Hf adatoms on Ir(111), we considered three atomic sites, the face-centered cubic (fcc), hexagonal close-packed (hcp), and vertically above an Ir substrate atom (atop), as the building units of the honeycomb lattice. Figure 3.3a demonstrates that Hf binding to the atop site is the weakest; relative to the atop site, the binding energies of the hcp and fcc sites are 1.54 and 1.28 eV/Hf, respectively. Next, we mixed the hcp, fcc, and atop sites to obtain three honeycomb structures, as found in Fig. 3.3b. Not surprisingly, the fcc/hcp mixing is 0.45 and 0.36 eV/Hf lower in energy than the atop/fcc and atop/hcp mixings, respectively.

Figure 3.4a illustrates a top view of the atomic structure for the fcc/hcp mixing on Ir(111), whereas Fig. 3.4b shows the corresponding simulated STM image for bias $= -1.5$ V. The honeycomb structure is clearly seen in the STM image as marked by the green hexagon. Figure 3.4c displays the corresponding experimental STM image. The overall features are in remarkable agreement with the simulated results in Fig. 3.4b.

A key issue here is whether Hf forms its own honeycomb lattice. While both the experimental STM images in Figs. 3.2b and 3.4c and the measured Hf–Hf distance strongly suggest so, more evidence comes from the calculated charge distribution in the Hf layer. Figure 3.5 depicts the total charge density in the Hf honeycomb plane. It reveals the formation of direct Hf–Hf bonds and thus explains why the Hf

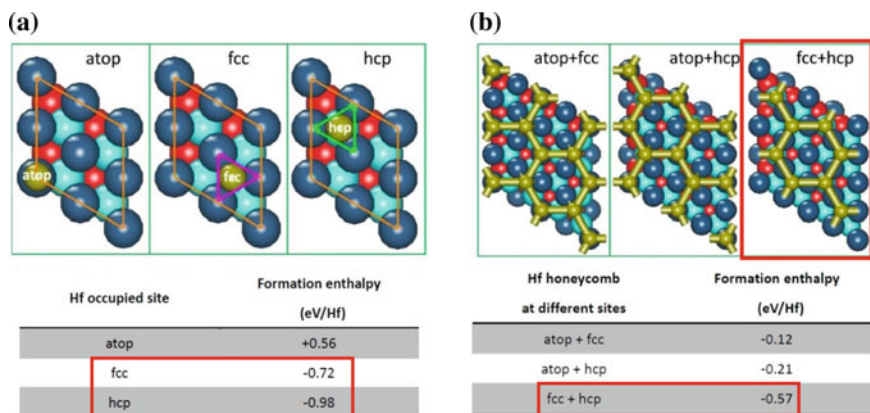


Fig. 3.3 Theoretical calculations for formation enthalpy of **a** single Hf atoms and **b** a layer of Hf honeycomb on Ir(111). Reproduced with permission from Ref. [14], © 2013 ACS

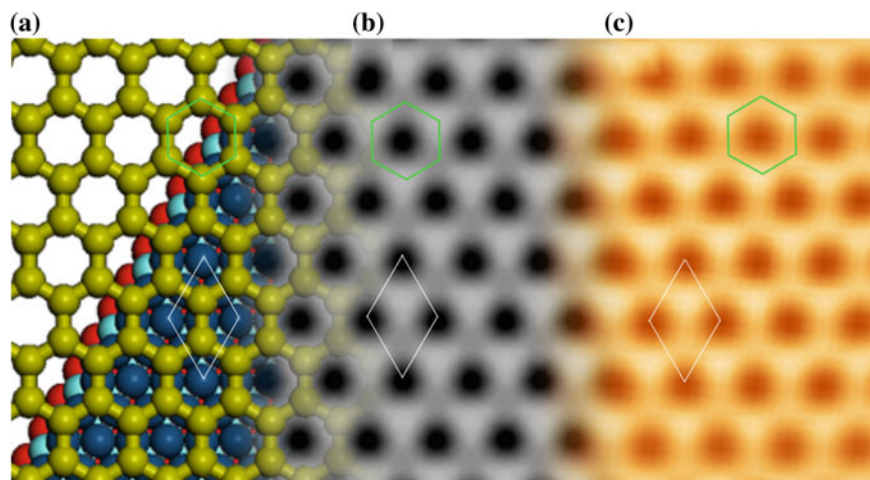


Fig. 3.4 Atomic configuration of Hf honeycomb lattice on Ir(111). **a** Top view of the calculated atomic structure. Half of the Hf atoms are on the fcc sites (vertically above the red Ir balls), while the other half are on the hcp sites (vertically above the cyan Ir balls). The white rhombus denotes the Ir(111) - (2×2) unit cell. **b** DFT-simulated STM image (-1.5 V). The Hf honeycomb is highlighted by the green hexagon. **c** Atomically resolved experimental STM image (-1.5 V, 0.1 nA) showing features identical to those in **(b)**. Reproduced with permission from Ref. [14], © 2013 ACS

does not merely follow the Ir triangular lattice. Another issue is whether Hf forms the honeycomb with Ir (in other words, forming surface alloys). Our calculations, as exhibited in Fig. 3.6, reveal that a honeycomb made of only Hf is energetically more stable than a honeycomb with Hf-Ir mixing. Therefore, both experiment and theory suggest the existence of a continuous single-layer Hf film with honeycomb

Fig. 3.5 The 2D charge density in the Hf plane on Ir(111) substrate. Reprinted with permission from Ref. [14], © 2013 ACS

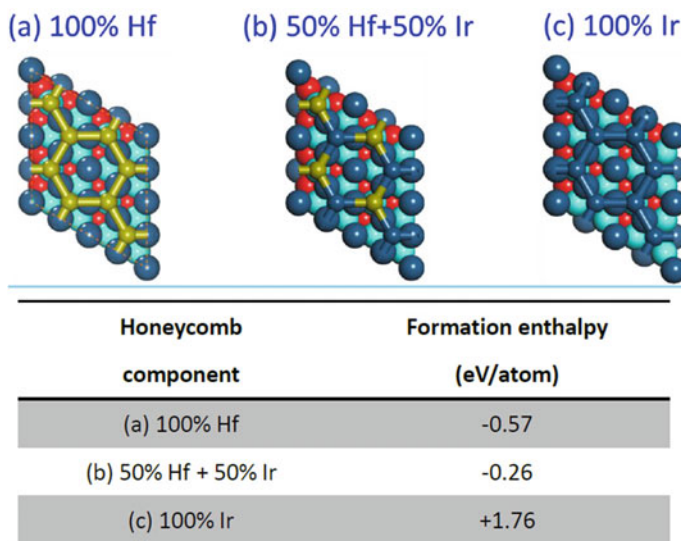
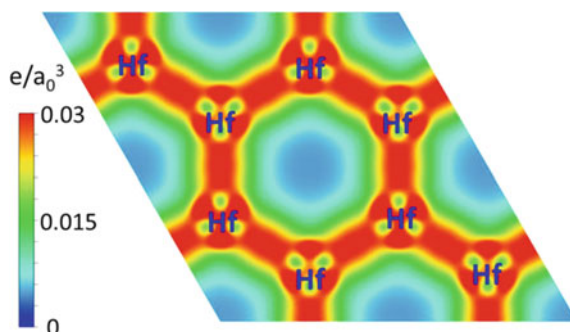


Fig. 3.6 Atomic models and formation enthalpy of honeycomb structures with different Hf–Ir mixing. Reproduced with permission from Ref. [14], © 2013 ACS

structure, supported on the Ir(111) substrate. The name of this material may be coined as “hafnene”, as a particular case of possible metalenes.

In light of the fact that freestanding honeycomb structures usually hold essential properties for technological applications, we have calculated the band structures of a freestanding Hf honeycomb. Figure 3.7 shows the band structures for (a) spin-up and (b) spin-down states. They reveal that the freestanding Hf honeycomb is metallic and strongly spin-polarized (and hence ferromagnetic), with a magnetic moment of 1.46 μ_B/Hf . The density of states (DOS) plots show the presence of a large number of d states near the Fermi level, which could be utilized for catalytic reactions [18]. Dirac cones also exist in this system. Because of the localization of the wave functions

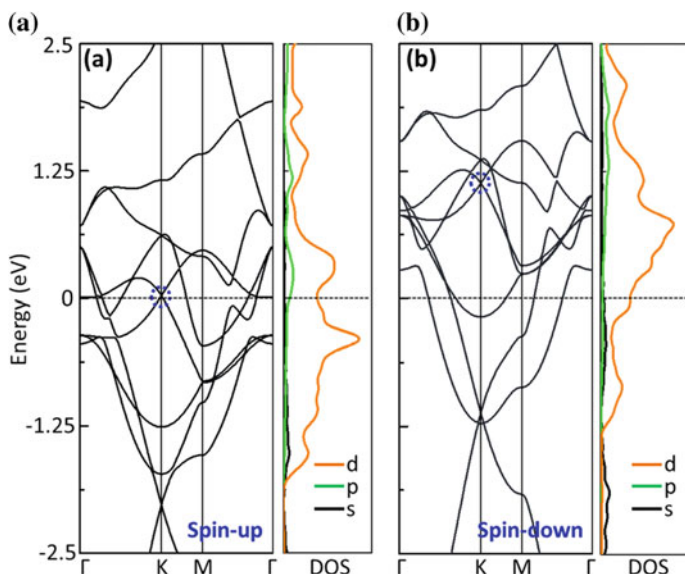


Fig. 3.7 Band structures of free-standing Hf honeycomb. **a** Spin-up and **b** spin-down states along with their partial densities of states. Dotted circles denote the positions of the Dirac cones near the Fermi level (set at $E = 0$). Reproduced with permission from Ref. [14], © 2013 ACS

in the 2D plane, which increases exchange coupling between electrons, the Dirac cone for the spin-down states is about 1 eV higher in energy than that for the spin-up states.

3.4 Bilayer Hafnene and Hafnene Grown on Other Supports

We observed the formation of a second Hf honeycomb layer on top of the first one upon increasing the Hf coverage, as shown in Fig. 3.8b. This could be important, as it suggests that the existence of the Hf honeycomb structure does not necessarily depend on the binding to the Ir substrate. Thus there comes a question that whether the single-layer Hf honeycomb structure could readily be separated from the substrate. It has not been possible so far, and even if separated, the freestanding film may not be stable. However, there may be other ways to isolate the Hf honeycomb structure from the substrate without strongly perturbing its physical properties or its physical integrity, for example, by intercalation [19–21].

What is more, it is necessary to note that the observation of Hf honeycomb on Ir(111) is not an isolated case. A similar honeycomb structure has also been fabricated on Rh(111) substrate, as revealed in Fig. 3.9 by LEED and STM.

Fig. 3.8 **a** Sub-monolayer and **b** bilayer hafnene. Adapted with permission from Ref. [14], © 2013 ACS

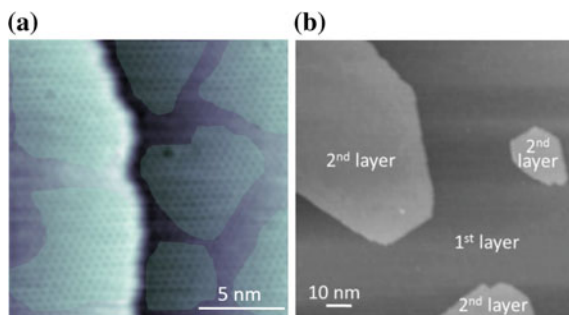
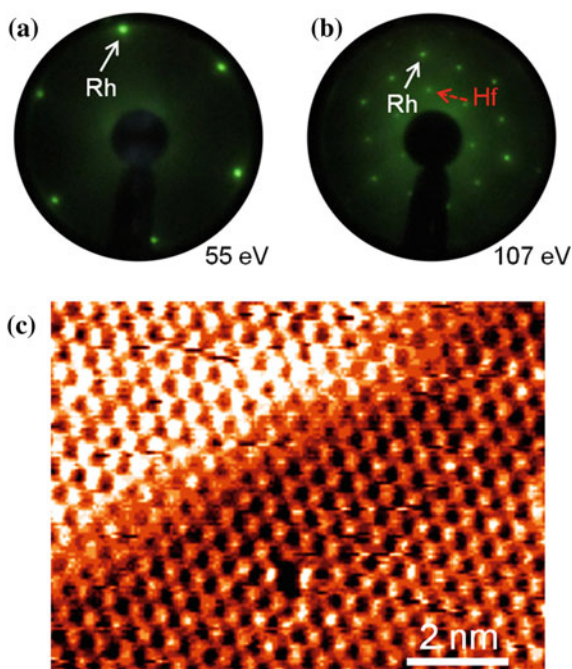


Fig. 3.9 LEED patterns of the Rh substrate **a** before and **b** after hafnene deposition. **c** The STM image of hafnene lattice on Rh(111). Reproduced with permission from Ref. [14], © 2013 ACS



3.5 Summary and Outlook

We report the first example of transition metal honeycomb structures-hafnene.

- (1) The LEED and STM studies reveal highly ordered Hf honeycomb lattices on Ir(111) substrates.
- (2) Interesting ferromagnetism, high density of d states at the Fermi level, and large spin-splitting of the Dirac cones are theoretically predicted for a freestanding Hf honeycomb structure.

- (3) Given the rich electronic, magnetic, and catalytic properties of TM elements in general, and the insufficiency of knowledge of their 2D structures, further realization and investigation of TM single layers are highly desirable. As the TM honeycomb structures provide a new platform to investigate hitherto unknown quantum phenomena and electronic behaviors in 2D systems, we expect them to have broad application potential in nanotechnology and related areas.

References

1. Corso M et al (2004) Boron nitride nanomesh. *Science* 303:217–220
2. Dean C et al (2010) Boron nitride substrates for high-quality graphene electronics. *Nat Nanotechnol* 5:722–726
3. Britnell L et al (2012) Field-effect tunneling transistor based on vertical graphene heterostructures. *Science* 335:947–950
4. Cahangirov S, Topsakal M, Akturk E, Sahin H, Ciraci S (2009) Two- and one-dimensional honeycomb structures of silicon and germanium. *Phys Rev Lett* 102:236804. <https://doi.org/10.1103/PhysRevLett.102.236804>
5. Liu C-C, Feng W, Yao Y (2011) Quantum spin hall effect in silicene and two-dimensional germanium. *Phys Rev Lett* 107:076802
6. Chen L et al (2012) Evidence for dirac fermions in a honeycomb lattice based on silicon. *Phys Rev Lett* 109:056804
7. Feng B et al (2012) Evidence of silicene in honeycomb structures of silicon on Ag(111). *Nano Lett* 12:3507–3511. <https://doi.org/10.1021/nl301047g>
8. Fleurence A et al (2012) Experimental evidence for epitaxial silicene on diboride thin films. *Phys Rev Lett* 108:245501. <https://doi.org/10.1103/PhysRevLett.108.245501>
9. Vogt P et al (2012) Silicene: compelling experimental evidence for graphenelike two-dimensional silicon. *Phys Rev Lett* 108:155501. <https://doi.org/10.1103/PhysRevLett.108.155501>
10. Tao L et al (2015) Silicene field-effect transistors operating at room temperature. *Nat Nanotechnol* 10:227–231. <https://doi.org/10.1038/nnano.2014.325>
11. Li L et al (2014) Buckled germanene formation on Pt(111). *Adv Mater* 26:4820–4824. <https://doi.org/10.1002/adma.201400909>
12. Mannix AJ, Kiraly B, Hersam MC, Guisinger NP (2017) Synthesis and chemistry of elemental 2D materials. *Nat Rev Chem* 1:0014. <https://doi.org/10.1038/s41570-016-0014>
13. Molle A et al (2017) Buckled two-dimensional Xene sheets. *Nat Mater* 16:163–169. <https://doi.org/10.1038/nmat4802>
14. Li LF et al (2013) Two-dimensional transition metal honeycomb realized: Hf on Ir(111). *Nano Lett* 13:4671–4674. <https://doi.org/10.1021/nl4019287>
15. Vanderbilt D (1990) Soft self-consistent pseudopotentials in a generalized eigenvalue formalism. *Phys Rev B* 41:7892
16. Kresse G, Furthmüller J (1996) Efficient iterative schemes for ab initio total-energy calculations using a plane-wave basis set. *Phys Rev B* 54:11169–11186. <https://doi.org/10.1103/PhysRevB.54.11169>
17. Perdew JP, Burke K, Ernzerhof M (1996) Generalized gradient approximation made simple. *Phys Rev Lett* 77:3865–3868. <https://doi.org/10.1103/PhysRevLett.77.3865>
18. Hammer B, Nørskov JK (2000) Theoretical surface science and catalysis—calculations and concepts. *Adv Catal* 45:71–129

19. Huang L et al (2011) Intercalation of metal islands and films at the interface of epitaxially grown graphene and Ru (0001) surfaces. *Appl Phys Lett* 99:163107
20. Meng L et al (2012) Silicon intercalation at the interface of graphene and Ir (111). *Appl Phys Lett* 100:083101
21. Li L, Wang Y, Meng L, Wu R-T, Gao H-J (2013) Hafnium intercalation between epitaxial graphene and Ir (111) substrate. *Appl Phys Lett* 102:093106